

Gamma-Ray Yield from Neutron Interactions with $^{10}\text{B}\dagger$

DONALD O. NELLIS, W. E. TUCKER, AND IRA L. MORGAN*

Texas Nuclear Corporation, Austin, Texas 78757

(Received 4 June 1969; revised manuscript received 29 September 1969)

Cross sections for γ rays produced by neutron bombardment of ^{10}B have been measured between 50 keV and 5 MeV and at 14.8 MeV. Special emphasis was placed on measurements of the 0.478-MeV γ ray from the $^{10}\text{B}(n, \alpha)^7\text{Li}$ reaction. Most of the unbound levels in ^{10}B did not emit any observable γ rays. The 0.478-MeV γ -ray production cross section showed a departure from $1/v$ above a neutron energy of 100 keV.

I. INTRODUCTION

BORON-10, comprising approximately 20% of naturally occurring boron and occupying the mid-position in the $1p$ -shell nuclei, is a complicated and interesting nucleus. It is perhaps best known for its large neutron-absorption cross section, the value of which is some ten times larger than the hydrogen-absorption cross section at thermal energies. This feature has led to its extensive use as a shielding material in and around accelerator and reactor facilities, where it is generally found in the form of "Boral" or some other borated compound. It is often used as a chemical shim in water-cooled nuclear power plants to control the neutron flux in the reactor core. It has long been used as a neutron-flux monitor in various neutron-detection instruments and is sometimes used as a neutron-flux standard. The cross section of interest in each of these applications is the $^{10}\text{B}(n, \alpha)^7\text{Li}$ reaction, which has a large (3837 b) cross section at thermal energies and follows an $E^{-1/2}$ dependence to about 100 keV.

In view of its extensive use, there is considerable interest¹ both in improved measurements of the $^{10}\text{B}(n, \alpha)^7\text{Li}$ reaction and in measurements of the γ rays produced in ^{10}B by its interaction with various energy neutrons. These latter measurements assist in the determination of basic nuclear structure and additionally provide important information for neutronics calculations used to determine reactor power losses and shielding requirements.

Although it is well known that the (n, α) reaction in ^{10}B produces two α groups and that a 0.478-MeV γ ray from the first excited state of ^7Li is associated with the second α group, few production cross-section measurements have been made for γ -ray emission from this excited state. Bichsel and Bonner² used a commercial BF_3 counter to make relative measurements of the (n, α) cross section between 20 keV and 4.8 MeV and normalized their data to an $E^{-1/2}$ extrapolation of the

thermal cross section at 20 keV. They were unable to resolve the two α groups in this experiment. Davis, Gabbard, Bonner, and Bass,³ using a grid-type ionization chamber, were able to measure cross sections for both the ground-state and first-excited-state α groups between 0.2 and 8.2 MeV. Cox,⁴ using the spherical shell transmission technique, measured the absorption cross section between 11 and 245 keV. The absorption cross section was measured indirectly by Mooring, Monahan, and Huddleston,⁵ who made simultaneous measurements of the total and integral scattering cross sections and obtained the quantity $\sigma_A = \sigma_T - \sigma_S$. Diment⁶ obtained similar results by measuring the total cross section and subtracting the scattering values of Mooring *et al.*⁵ More recently, Macklin and Gibbons⁷ determined the $^{10}\text{B}(n, \alpha_0)^7\text{Li}$ cross section between 30 and 500 keV by reciprocity from the inverse reaction and determined the corresponding $^{10}\text{B}(n, \alpha_1)^7\text{Li}^*$ cross sections using the α_0/α_1 branching ratios.^{7,8} Bogart and Nichols⁹ made relative cross-section measurements of the $^{10}\text{B}(n, \alpha)^7\text{Li}$ reaction with a BF_3 proportional counter and normalized their data to an $E^{-1/2}$ variation of the thermal cross section below 80 keV. In this work, we have measured the production of γ rays from (n, p) , (n, α) , and (n, n') interactions, using incident neutrons between 45 keV and 5 MeV and at 14.9 MeV. One angular distribution measurement was made at 4 MeV. Special emphasis was placed on the measurement of the yield of the 0.478-MeV γ ray from the $^{10}\text{B}(n, \alpha_1)^7\text{Li}^*$ reaction at neutron energies up to 1 MeV in order to determine any deviation from the $E^{-1/2}$ dependence of the cross section described by $572/E^{1/2}$ (E in eV).⁶

³ E. A. Davis, F. Gabbard, T. W. Bonner, and R. Bass, *Nucl. Phys.* **27**, 448 (1961).

⁴ S. A. Cox, Conference on Neutron Cross Section Technology, Washington, D. C., 1966, edited by P. B. Hemming, p. 701 (unpublished).

⁵ F. P. Mooring, J. E. Monahan, and C. M. Huddleston, *Nucl. Phys.* **82**, 16 (1966).

⁶ K. M. Diment, Atomic Energy Research Establishment Report No. AERE-R5224, 1967 (unpublished).

⁷ R. L. Macklin and J. H. Gibbons, *Phys. Rev.* **165**, 1147 (1968).

⁸ R. L. Macklin and J. H. Gibbons, *Phys. Rev.* **140**, B324 (1965).

⁹ D. Bogart and L. L. Nichols, NASA Technical Report No. NASA TN D-4783, 1968 (unpublished); *Nucl. Phys.* **A125**, 463 (1969).

[†] Research supported by the U.S. Atomic Energy Commission.

* Present address: Physics Department, University of Texas, Austin, Tex.

¹ Compilation of EANDC Requests, Report No. EANDC 55 U, 1966 (unpublished).

² H. Bichsel and T. W. Bonner, *Phys. Rev.* **108**, 1025 (1957).

TABLE I. Cross sections for production of γ rays from neutron bombardment of ^{10}B . The 0.478-MeV γ ray is listed separately in Table II. The cross section at 14.8 MeV for the 0.410-MeV γ ray was obtained indirectly, as explained in the text. Errors shown include statistics, background, and attenuation correction errors and an estimated 5% error in the long-counter efficiency.

E_γ (MeV)	$d\sigma(55^\circ)/d\Omega$ (mb/sr)										
	0.410	0.717	1.02	1.43	2.15	2.60	2.86	3.01	3.37	4.44	6.04
1.45 ± 0.05		0.31 ± 0.04									
1.60 ± 0.05		0.87 ± 0.06									
1.72 ± 0.04		0.89 ± 0.06									
1.80 ± 0.04		1.50 ± 0.10									
1.97 ± 0.04		3.47 ± 0.24									
3.10 ± 0.15		4.51 ± 0.27									
3.50 ± 0.10		4.95 ± 0.31	1.11 ± 0.09		0.70 ± 0.06						
4.00 ± 0.05		4.87 ± 0.30	1.69 ± 0.12	0.82 ± 0.06	0.83 ± 0.10						
4.90 ± 0.07	0.63 ± 0.15	7.39 ± 0.44	2.31 ± 0.14	1.26 ± 0.08	1.55 ± 0.09		1.70 ± 0.10		1.16 ± 0.07		
14.8 ± 0.4	0.21 ± 0.04	2.48 ± 0.12	0.74 ± 0.04	0.69 ± 0.04	0.57 ± 0.03	0.74 ± 0.04	0.51 ± 0.04	0.39 ± 0.03	1.68 ± 0.08	0.85 ± 0.05	0.28 ± 0.04

II. EXPERIMENTAL

Monoenergetic neutrons were obtained from the Texas Nuclear 3-MeV Van de Graaff, using the $\text{T}(p, n)^3\text{He}$, $\text{D}(d, n)^3\text{He}$, and $\text{T}(d, n)^4\text{He}$ reactions. The targets used were as follows: For measurements between 50 and 700 keV, the target consisted of a tritium-loaded titanium layer ($200 \mu\text{g}/\text{cm}^2$) containing approximately $125 \text{ mCi}/\text{cm}^2$ of tritium mounted on a 10-mil-thick copper backing. Between 700 keV and 2 MeV, a similar target with a titanium layer ($\sim 1 \text{ mg}/\text{cm}^2$), containing approximately $800 \text{ mCi}/\text{cm}^2$ of tritium, was used. The 3–5-MeV measurements were made using a gas target consisting of a 1-cm-long cell filled to a pressure of 1 atm with deuterium gas and separated from the accelerator vacuum by a 0.1-mil Mo foil. The 14.8-MeV measurements used a tritium loaded titanium target identical to that used for the 700-keV–2-MeV measurements.

The energy spreads in the neutron beam incident on the scattering samples are shown in Tables I and II. For incident neutron energies above 300 keV, the scattering samples were positioned at 0° with respect to the direction of the incident charged-particle beam, so that the principal source of energy spread is due to the target thickness. For the thinner tritium targets used for measurements up to 700 keV, the target thickness for incident protons was 26 keV for the lowest energy protons used, resulting in a neutron-energy spread of ± 16 keV for 300-keV neutrons. The distribu-

tion of tritium in the targets had been investigated previously as part of another project and was found to vary by about 15%. Investigation likewise did not reveal any evidence for diffusion of tritium into the copper backing, so that the target thickness is defined by the

TABLE II. Cross sections for the 0.478-MeV γ ray from the $^{10}\text{B}(n, \alpha_1\gamma)^7\text{Li}$ reaction. The measured 55° cross sections have been multiplied by 4π to yield the integrated cross sections in the Table.

E_n (MeV)	$\sigma(n, \alpha_1\gamma)$ (mb)	E_n (MeV)	$\sigma(n, \alpha_1\gamma)$ (mb)
0.047 ± 0.022	2982 ± 209	0.99 ± 0.05	214 ± 13
0.077 ± 0.022	1941 ± 136	1.09 ± 0.05	204 ± 13
0.087 ± 0.022	2041 ± 143	1.20 ± 0.05	167 ± 10
0.120 ± 0.022	1731 ± 121	1.30 ± 0.05	104 ± 6
0.171 ± 0.020	1598 ± 112	1.45 ± 0.05	111 ± 7
0.224 ± 0.020	1320 ± 79	1.60 ± 0.05	84 ± 5
0.300 ± 0.016	1095 ± 68	1.72 ± 0.04	115 ± 7
0.350 ± 0.015	951 ± 59	1.80 ± 0.04	146 ± 9
0.406 ± 0.015	827 ± 51	1.97 ± 0.04	165 ± 10
0.450 ± 0.014	801 ± 50	3.10 ± 0.15	95 ± 6
0.502 ± 0.013	679 ± 42	3.50 ± 0.10	101 ± 6
0.550 ± 0.011	637 ± 40	4.00 ± 0.05	127 ± 8
0.601 ± 0.012	561 ± 35	4.90 ± 0.07	88 ± 5
0.703 ± 0.011	419 ± 26	14.8 ± 0.4	34 ± 3
0.76 ± 0.05	417 ± 26		
0.85 ± 0.05	266 ± 16		
0.95 ± 0.05	267 ± 16		

tritium-absorbing titanium layer. For incident energies below 300 keV, the scattering samples were placed at various angles to the incident proton beam, and an additional angular-dependent energy spread of the source neutrons was added to the spread produced by the target thickness. Background neutrons from the $^{65}\text{Cu}(p, n)^{65}\text{Zn}$ reaction, produced by protons passing through the target's titanium layer into the copper backing, were also investigated. The yield of the copper neutrons was negligible except at one bombarding energy. At a bombarding energy corresponding to 1.97-MeV neutrons (see Table II), the yield of neutrons from the copper reaction was of the order of 1.4% of the measured neutron yield. Since the copper neutrons are not monoenergetic at this bombarding energy, it is difficult to determine their effect on the cross section. It is estimated that they could be responsible for as much as 20 mb of the cross section reported in Table II for 1.97-MeV neutrons.

Scattering samples consisted of isotopically enriched (92.2%) ^{10}B , obtained from Oak Ridge National Laboratory. The chemical analysis supplied listed the following impurities: C, 2%; ^{11}B , 2.6%; metals, 1.3%; O and N, <1.09%. The samples, in the form of right circular cylinders encased in 3-mil Mylar film, were used in three sizes: 3.95 cm diam \times 6.0 cm, 2.5 cm diam \times 5.08 cm, and 2.0 cm diam \times 4.0 cm.

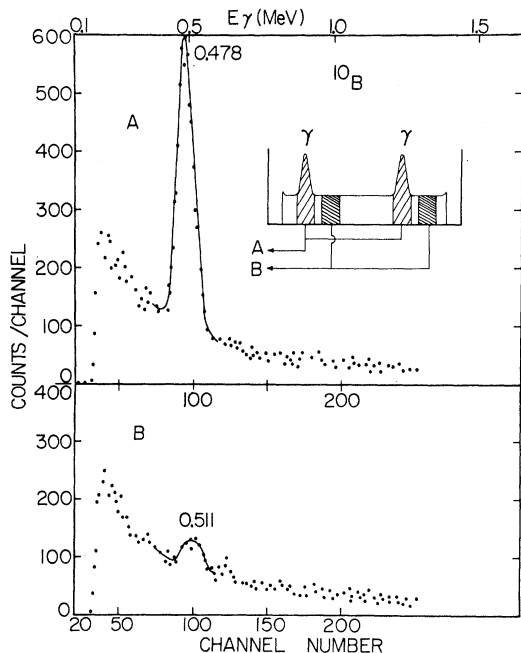


FIG. 1. γ -ray spectra obtained from ^{10}B bombarded with 120-keV neutrons. Insert shows a time-of-flight spectrum and the method of positioning the foreground and background gates. Upper spectrum is associated with the foreground gates marked A and the lower spectrum is associated with the background gates marked B. Failure to observe the 0.478-MeV peak in the lower spectrum indicates that thermal and room-scattered neutron interactions with the scattering sample are negligible.

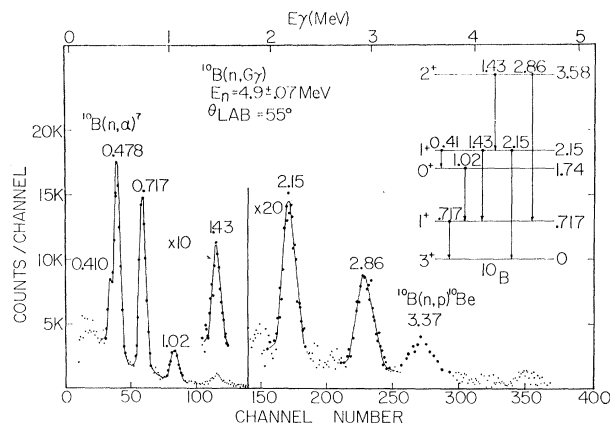


FIG. 2. γ -ray spectrum from ^{10}B using 4.9-MeV incident neutrons. Origin of the peaks arising from inelastic neutron scattering are indicated on the level diagram. Two other peaks, arising from (n, α) and (n, p) reactions, are labeled.

The experimental equipment used in this work (and described elsewhere)^{10,11} consists basically of a two-crystal anticoincidence γ -ray spectrometer operated in conjunction with conventional time-of-flight techniques. In most cases, the foreground, associated with prompt γ -ray peaks in the time-of-flight spectrum, and the background, associated with the time-independent portion of the time-of-flight spectrum, were accumulated simultaneously. This was accomplished by gating the analyzer with one pair of windows set on the prompt peaks in the time-of-flight spectrum and with another pair on the random portion of the spectrum. The linear spectrum associated with each pair of gates was routed to separate sections of the analyzer memory. Figure 1, showing the foreground and background spectra taken at an incident energy of 120 keV, illustrates the gating used on the time-of-flight spectrum and the linear spectrum associated with each pair of gates. The double presentation of the γ -ray peaks in the time-of-flight spectrum is characteristic of the current system.¹⁰

The present experiment made use of a NaI(Tl) crystal as the center detector in the spectrometer, but some measurements were taken with a Ge(Li) center detector to check for possible additional unresolved γ rays. At neutron energies above 300 keV, the scattering samples were placed at 0° to the accelerator-beam tube at some 5–8 cm from the neutron-producing target. Below 300 keV, the scattering samples were placed at the same distance but at various angles to the beam tube. The γ -ray detector was placed at 55° to a line drawn from the neutron target to the scatterer. The neutron flux incident on the scattering samples was determined from a calibrated polyethylene long counter placed directly behind the scattering samples at 150 cm

¹⁰ J. B. Ashe, I. L. Morgan, and J. D. Hall, Rev. Sci. Instr. **37**, 1559 (1966).

¹¹ G. H. Williams and I. L. Morgan, Nucl. Instr. Methods **45**, 313 (1966).

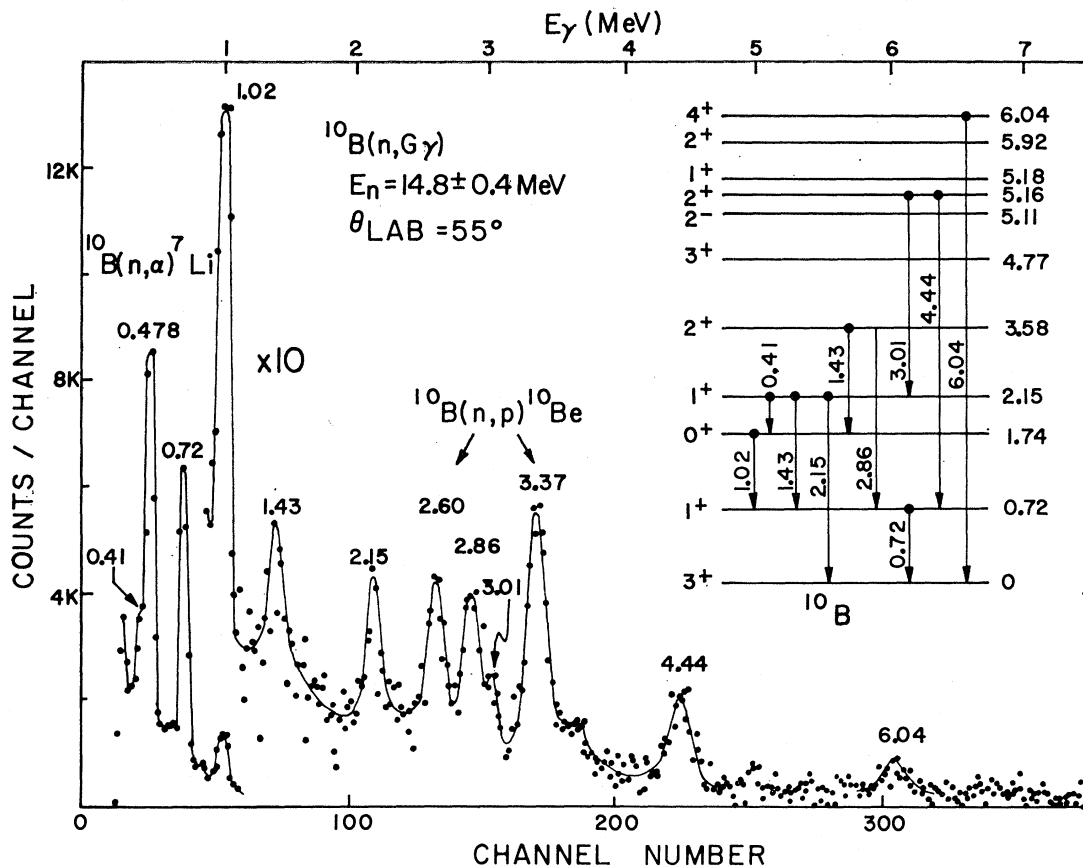


FIG. 3. γ -ray spectrum from ^{10}B , using 14.8-MeV incident neutrons. Transitions produced by inelastic scattering are shown on the level diagram. Two peaks produced by the (n, p) reaction and one from the (n, α) reaction are also shown.

from the neutron source along a line defined by the neutron target and the scattering samples. The polyethylene long counter used in these measurements was of standard size, having polyethylene in place of the usual paraffin, and had a response function similar to that reported in the literature.¹² The response function was obtained by direct comparison with proton-recoil telescope measurements between 1.5 and 5 MeV and at 14.8 MeV.

At the end of each data run, corrections were obtained for the long-counter measurement. These consisted of scatterer-in-versus-scatterer-out measurements and a background measurement taken with a 40-cm-long iron shadow cone between the long counter and the neutron target. After correcting the long-counter measurement for background and for sample absorption and scattering, the measurement was converted to a neutron flux by means of a long-counter efficiency curve determined down to 1.5 MeV by comparison with proton-recoil

telescope measurements. For measurement of neutrons below 1 MeV the relative long-counter response curve of Allen and Ferguson,¹² normalized to our long-counter efficiency curve at 1.5 MeV, was used.

The neutron flux at the midpoint of the scattering sample with the sample not in place was first calculated using the long-counter measurements just described. An effective neutron flux with the scatterer in place was then determined by correcting the no sample flux for sample attenuation, using the method of Cranberg and Levin,¹³ and for geometry effects associated with the finite size of the scatterer. In the corrections for sample attenuation, the nonelastic cross sections of Diment⁶ rather than the total cross sections were then used since single elastic events neither appreciably degrade the neutron energy nor effectively remove neutrons from the beam. Since the effective neutron flux determined by the method indicated above can be altered by multiple scattering in the sample, calculations were made to determine the magnitude of this effect. For

¹² W. D. Allen and A. T. G. Ferguson, in *Fast Neutron Physics*, edited by J. B. Marion and J. L. Fowler (Wiley-Interscience, Inc., New York, 1960), pp. 372-373.

¹³ L. Cranberg and J. S. Levin, Los Alamos Scientific Laboratory Report No. LA-2177, 1959 (unpublished).

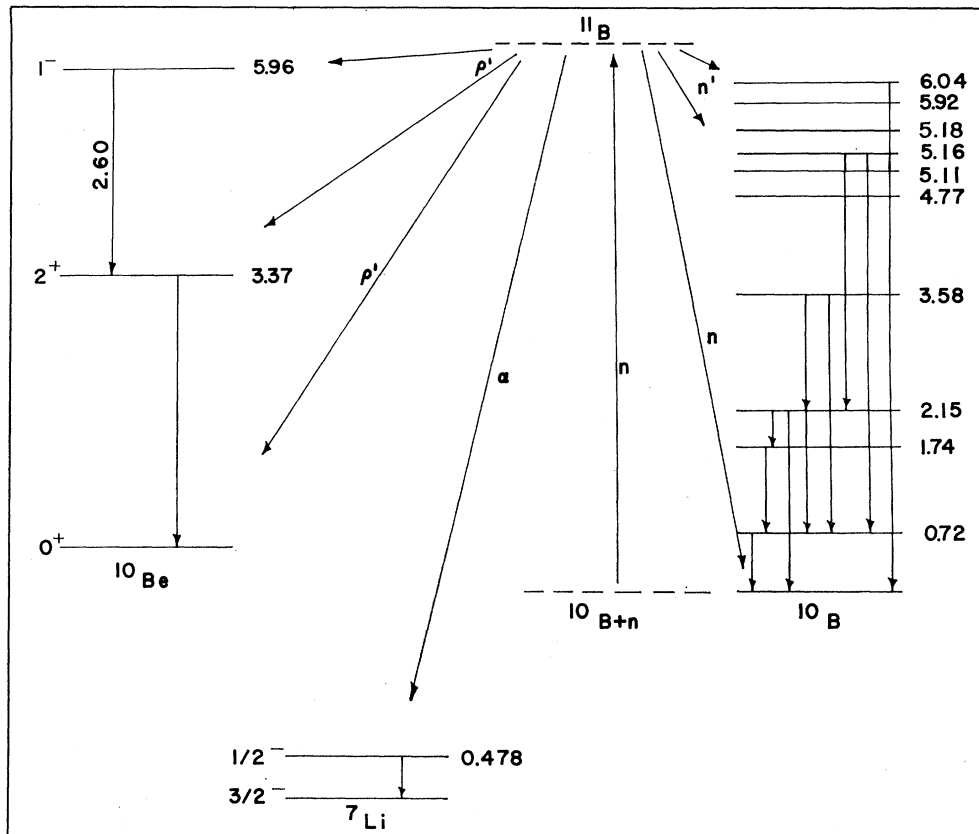


FIG. 4. Schematic representation of the reactions giving rise to the observed γ rays. The compound nucleus ^{11}B emits protons (p), α particles (α), or reemits neutrons (n). Symbol (n') indicates inelastic neutron emission.

incident neutron energies below the inelastic threshold near 800 keV, only elastic events can contribute to multiple scattering. At higher incident neutron energies, the inelastic cross section is low, and multiple inelastic scattering effects should be small. Calculations using the scattering and absorption cross sections of Diment⁶ indicate that a second scattering of nonelastic character by neutrons that have elastically scattered once increases the effective neutron flux by approximately 2% at 50 keV and 2.6% at 500 keV. Calculations for higher incident energy neutrons were not undertaken because of the lack of reliable elastic and absorption cross sections, but estimates indicate a 2–3% increase in the effective flux at these energies. The effects of the multiple-scattering calculations have not been included explicitly in the values listed in Tables I and II, but they are included as part of the attenuation error discussed in the Sec. III. The raw γ -ray spectra were analyzed in variable energy increments and corrected for self-attenuation of the γ rays by the scattering sample for detector efficiency and for Compton scattering produced by γ rays above the energy increment under analysis.

III. RESULTS AND DISCUSSION

Typical γ -ray spectra obtained are shown in Figs. 1–3. The observed γ -ray peaks correspond to known¹⁴ γ -ray transitions in ^{10}B plus additional peaks arising from excited states in ^{10}Be and ^7Li populated through (n, p) and (n, α) reactions. Figure 4 indicates schematically the various reaction channels observed in this experiment. The level schemes and level information shown on Figs. 2–4 were taken from the compilation of Ajzenberg-Selove and Lauritsen,¹⁴ with the exception of the assignment of the 4.77-MeV level, which was taken from the work of Alburger *et al.*¹⁵

The strong peak observed at 0.478 MeV in Figs. 1–3 comes from the first excited state of ^7Li produced by the (n, α) reaction and will be discussed in greater

¹⁴ F. Ajzenberg-Selove and T. Lauritsen, Nucl. Phys. **11**, 1 (1959); *Nuclear Data Sheets*, compiled by K. Way *et al.* (Printing and Publishing Office, National Academy of Sciences—National Research Council, Washington, 25, D.C., 1961), NRC 61-5, 6-91.

¹⁵ D. E. Alburger, P. D. Parker, D. J. Bredin, D. H. Wilkinson, P. F. Donovan, A. Gallman, R. E. Pixley, L. F. Chase, and R. E. McDonald, Phys. Rev. **143**, 692 (1966).

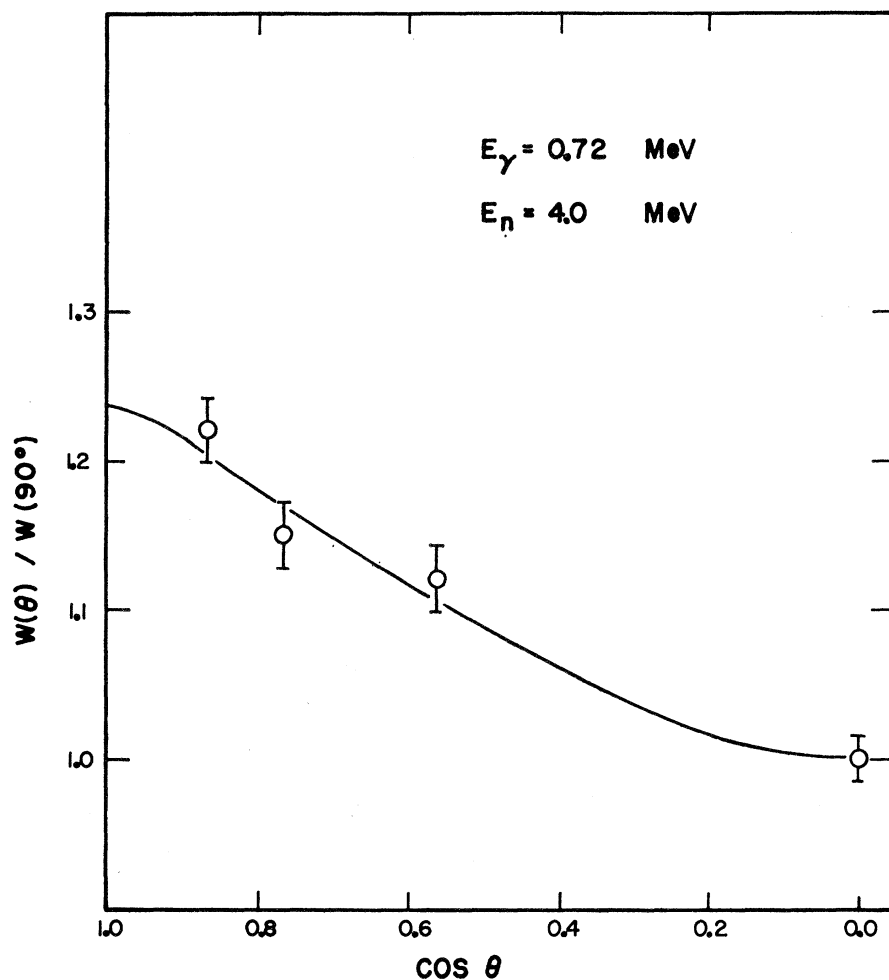


FIG. 5. Angular distribution of the 0.72-MeV γ ray at a bombarding energy of 4 MeV. Error bars include statistics and normalization errors.

detail below. The peak at 3.37 MeV in Figs. 2 and 3 comes from the first excited level of ^{10}Be produced by the (n, p) reaction. Also produced by the (n, p) reaction, the γ peak at 2.6 MeV in Fig. 3 comes from a transition between the 5.96- and 3.37-MeV levels in ^{10}Be . The ground-state transition from the 5.96-MeV level in ^{10}Be , if present, is obscured by the 6.05-MeV transition in ^{10}B . The 55° differential cross sections for the observed γ rays, with the exception of the 0.478-MeV peak, are given in Table I. The 0.478-MeV cross sections are tabulated separately in Table II. Errors shown in the tables consist of a 1.5% error in the neutron-flux background, a 3% error in the combined attenuation and anisotropy correction, a 5% error in the long-counter efficiency, and the statistical errors obtained from the data.

Although the 0.410-MeV γ -ray peak was not completely resolved in either Fig. 2 or Fig. 3, we were able to obtain a cross section at 4.9 MeV (Fig. 2) by the stripping of known line shapes. At 14.8 MeV (Fig. 3), this was not practical, and the cross section¹ listed in Table I

is an estimate obtained by multiplying the 4.9-MeV cross section by a factor (0.331) that is the average of the ratios of the 14.8–4.9-MeV cross sections of the 0.717-, 1.02-, 2.15-, and 2.86-MeV γ rays. A comparison of the γ -ray branching ratios from the 2.15- and the 3.58-MeV states of ^{10}B with the results reported in the literature^{14,16} is complicated by the fact that both levels decay with the emission of a 1.43-MeV γ ray. Nevertheless, the ratio of the 2.15–0.410-MeV γ rays from the level at 2.15 MeV is seen from Table I to be approximately 3:1 at both 4.9- and 14.8-MeV neutron bombarding energies, whereas other investigators report 1:1¹⁴ and 2:1¹⁶ for this ratio.

No evidence for a ground-state transition from the 3.58-MeV level in ^{10}B was observed at 4.9 MeV, as seen in Fig. 2. At 14.8 MeV, a broad peak observed on the high side of the 3.37-MeV peak in Fig. 3 could be attributed to this transition or possibly to a transition from

¹⁶ R. E. Segel, P. P. Singh, S. S. Hanna, and M. A. Grace, Phys. Rev. **145**, 736 (1966).

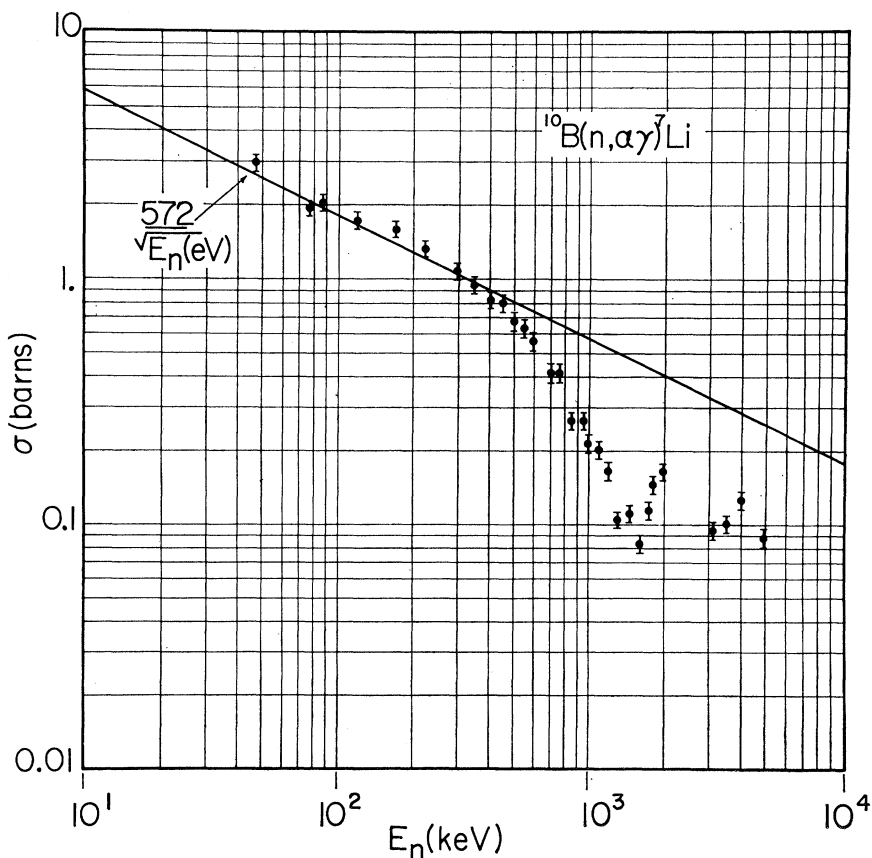


FIG. 6. The yield of the 0.478-MeV γ ray from the $^{10}\text{B}(n, \alpha)^7\text{Li}^*$ reaction. The solid line represents the $E^{-1/2}$ dependence of this reaction obtained from the absorption cross section $611/E^{1/2}$ (E in eV) and the thermal branching ratio due to Macklin and Gibbons (Ref. 7). Error bars are shown on the points, and their values are given in Table II. Plotted points are absolute values. No normalization was used.

the 3.56-MeV level in ^6Li , excited by α emission from unbound states in ^{10}B . The ground-state transition from the 5.16-MeV ^{10}B level was not observed, but this is expected since the branching ratio is reported^{15,16} to be only 5%. Also, no γ rays were observed from levels at 4.77, 5.11, 5.18, and 5.92 MeV, as expected, since these are all unbound levels lying above the α -emission threshold at 4.46 MeV and are thought to decay 100% by α emission. Alburger *et al.*¹⁵ have measured the α - and γ -branching ratios for the 4.77- and 5.16-MeV levels, and they found that the 4.77-MeV level decays 99.8% by α emission but that the 5.16-MeV level decays only 13% by this mode. Segel *et al.*¹⁶ found the α -emission branching ratio of the 5.16-MeV level to be 27%. These values seem consistent with the present results, which indicate (Fig. 3) no emission from the 4.77-MeV level and γ -ray transitions of 3.01 and 4.44 MeV from the 5.16-MeV level. The large γ -to- α -ray ratio from this unbound state is attributed to its $T=1$ character, which strongly inhibits α emission.

The 4.44-MeV γ -ray cross section listed in Table I has been corrected for contributions from two other sources. The original experimental results included a 0.475-mb/sr contribution from the 4.43-MeV level in carbon, present as a 2% impurity in the sample and as a

0.6% constituent of the Mylar film containing the samples. An additional contribution amounting to 0.078 mb/sr from the 4.46-MeV level in ^{11}B , present as a 2.6% impurity in the sample, was also included. The contributions from each of these sources were calculated from known cross sections and subtracted from the original yield. After these corrections, the results of Table I yield branching ratios of 56 and 44% for the 3.01- and 4.44-MeV γ transitions from the 5.16-MeV level compared to 69 and 31% obtained by Alburger¹⁵ and 72 and 28% obtained by Segel.¹⁶

The 6.04-MeV γ peak (Fig. 3) is the ground-state transition from the $J^\pi=4^+$, $T=0$ level at 6.04 MeV. This level has been studied¹⁷⁻²¹ extensively by inelastic scattering of protons, deuterons, α particles, and electrons and reportedly has an α width of 90 ± 4 eV²⁰ and a γ width of 0.12 ± 0.02 eV.²¹ Its decay mode is predom-

¹⁷ G. Schrank, E. K. Warburton, and W. W. Daehnick, Phys. Rev. **127**, 2159 (1962).

¹⁸ D. Hasselgren, P. V. Renberg, O. Sundberg, and G. Tibell, Nucl. Phys. **69**, 81 (1965).

¹⁹ B. H. Armitage and R. E. Meads, Nucl. Phys. **33**, 494 (1962).

²⁰ V. Meyer, R. E. Pixley, and P. Truol, Nucl. Phys. **A101**, 321 (1967).

²¹ G. Fricke, G. R. Bishop, and D. B. Isabelle, Nucl. Phys. **67**, 187 (1965).

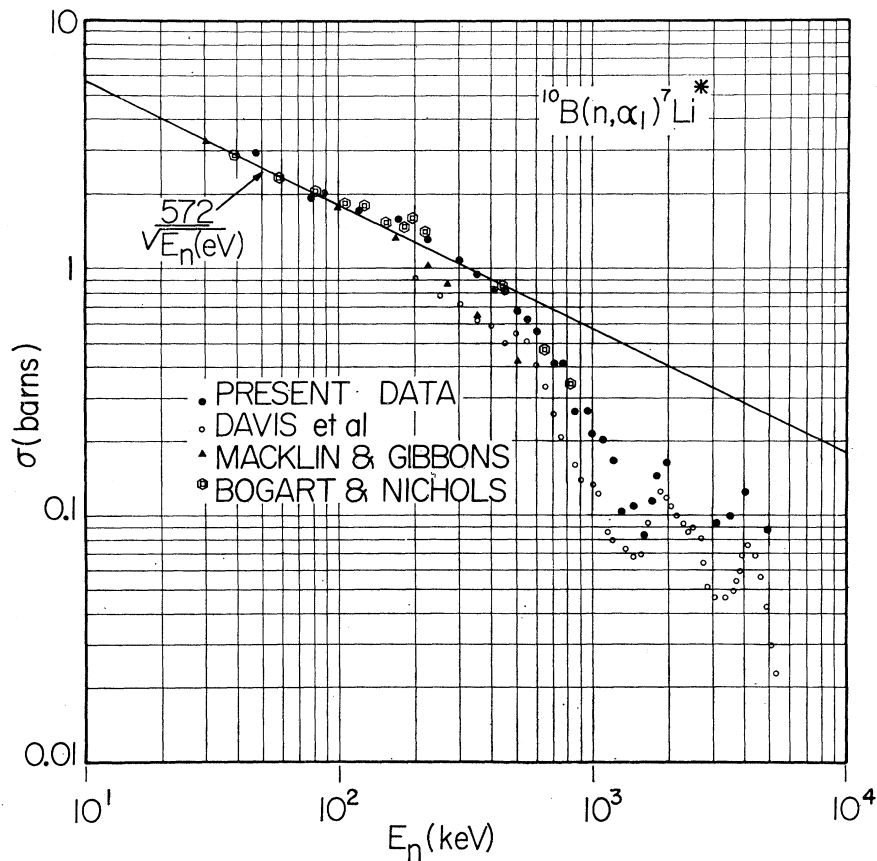


FIG. 7. Comparison of the $^{10}\text{B}(n, \alpha)^7\text{Li}^*$ cross section with the results of other experimenters. Macklin and Gibbons (Ref. 7) normalized their data to the $E^{-1/2}$ variation at 30 keV. Bogart and Nichols (Ref. 9) fitted their data to the $E^{-1/2}$ line below 80 keV. [Note that their (n, α) shown here was obtained from their total α measurement as described in the text.] Results of Davis *et al.* (Ref. 3) and present results are based on neutron-flux determination. No normalization to $E^{-1/2}$ was used.

inantly to the ground state²² (in agreement with our observations) by $E2$ radiation, indicating some form of collective excitation of the level.^{17,21,22}

At $E_n = 4$ MeV, γ -ray spectra were measured at angles of 30° , 40° , 55° , and 90° . Angular distributions were obtained for the 0.478-, 0.72-, and 1.02-MeV γ rays. The distribution of the 0.478- and 1.02-MeV γ rays were isotropic as expected since they originate from levels of spin $\frac{1}{2}$ and 0, respectively. The distribution of the 0.72-MeV γ ray, shown in Fig. 5, has an anisotropy of approximately 1.24, consistent with an $E2$ transition and in reasonable agreement with correlation measurements of others.^{23,24}

The predominant reaction at low neutron bombarding energies is the (n, α) reaction, leading to the ground and first excited states of ^7Li . The 0.478-MeV γ ray from the excited state was measured over a wide range of neutron energies, and the results are plotted in Fig. 6. A typical foreground and background spectrum taken at $E_n = 120$ keV, shown in Fig. 1, shows no evidence for thermal excitation of this γ ray because of background neutrons. The γ -ray distribution is isotropic since the

spin of the 0.478-MeV level is $\frac{1}{2}$. The results, plotted in Fig. 6, are the integral cross sections equal to 4π times the measured 55° differential cross sections. The integral cross sections, along with their estimated errors and errors in the incident neutron energy, are listed in Table II. The cross-section values shown in Table II and on Fig. 6 are absolute values based on neutron-flux determination made with a calibrated long counter. No attempt was made to fit the data to the $E^{-1/2}$ line shown in Fig. 6.

In Fig. 7, the cross sections obtained in the present experiment through measurement of the 0.478-MeV γ ray are compared with the results of other experimenters using different techniques. Two of these^{3,9} measured the α -particle yield directly, and another⁷ obtained the results by reciprocity, using the inverse reaction. Davis *et al.*³ obtained cross sections for the excited-level α group directly, using a gridded ion chamber. Bogart and Nichols⁹ obtained relative cross sections for the total α yield and normalized their results by fitting the relative data to an $E^{-1/2}$ variation below 80 keV. For the relative cross-section measurements, these authors used a precision long-counter (PLC)²⁵ neutron monitor

²² L. Meyer-Schutzmeister and S. S. Hanna, Phys. Rev. **108**, 1506 (1957).

²³ S. M. Shafroth and S. S. Hanna, Phys. Rev. **95**, 86 (1954).

²⁴ R. R. Carlson and E. B. Nelson, Phys. Rev. **98**, 1310 (1955).

²⁵ J. DePangher and L. L. Nichols, Battelle-Northwest Report No. BNWL-260, 1966 (unpublished).

whose relative efficiency response between 30 keV and 1 MeV differs somewhat from the response of the long counter used by us. We have taken the total α cross sections of Bogart and Nichols⁹ and converted them to (n, α_1) cross sections, using the branching ratios of Macklin and Gibbons⁷ below 450 keV and of Davis *et al.*³ above 450 keV. The results are plotted on Fig. 7. Our present results are in agreement with those of Bogart and Nichols in the region where they overlap. Both sets of data lie above the $E^{-1/2}$ line in the region between 100 and 300 keV and are indicative of a broad resonance in the neutron-absorption cross section. The state in ^{11}B near 11.68 MeV, having a reported¹⁴ width of 140 keV and corresponding to an incident energy around 230 keV, is believed to be responsible for this variation in the $E^{-1/2}$ dependence. Mooring *et al.*⁵ have observed this same broad resonance structure in both the total and absorption cross sections. Experimental values below 100 keV appear to be in agreement, but above 200 keV our results and those of Bogart and Nichols⁹ are approximately 50% larger than the values of Macklin and Gibbons⁷ and Davis *et al.*³ The absorption cross sections of Diment⁶ have been treated with the same branching ratios that were used on the data of Bogart and Nichols. While the results are not plotted on Fig. 7, they are essentially in agreement with Davis *et al.*³ and Macklin and Gibbons.⁷

IV. CONCLUSIONS

On the basis of data presented, it is concluded that the $^{10}\text{B}(n, \alpha_1)^7\text{Li}^*$ reaction varies as $E^{-1/2}$, up to an energy of 100 keV. From 100 to 300 keV, the cross section lies above the $E^{-1/2}$ line because of a broad resonance situated near 11.68 MeV in ^{11}B . Above 300 keV, the reaction gives values lying below the $E^{-1/2}$ line. The different methods used to determine the neutron flux possibly explain the discrepancy between the present measurements and those of Davis *et al.*³ The long counter of Davis was calibrated absolutely by comparison with a calibrated Pu-Be source, while our long counter was calibrated by means of a proton-recoil telescope. The quoted uncertainty of Davis's data is 20%, but the $^{10}\text{B}(n, t2\alpha)$ cross sections included in the same report are much lower than those reported by others,^{5,6} so

that the uncertainty may be larger than the reported 20%.

The values of Macklin and Gibbons (Fig. 7) are extremely dependent on accurate branching ratios for the two α groups. The variations found among different measurements of these ratios⁷ are not large enough to account for the disagreement with the present results in the region above 200 keV. Additional high-precision measurements are needed in the region 100–300 keV to determine the exact shape of the broad resonance there before this reaction can be used as a neutron-flux standard above 100 keV.

An attempt to compare our 14.8-MeV results with the reported²⁷ 14-MeV nonelastic cross section of 560 mb was made as follows: Since most γ -ray distributions can be represented by a polynomial of the form $W = A_0 + A_2 P_2(\cos\theta)$, the integrated cross section is essentially 4π times the 55° differential cross section. Then, from Table I, one obtains from the 0.72-, 2.15-, 3.37-, and 6.04-MeV transitions (all other γ rays are cascades and are included in these four) a yield of 62.9 mb that, coupled with the 0.478-MeV γ yield of Table II, gives a total γ -ray production of 96.9 mb. The α -emission yield from unbound levels at 4.77, 5.11, 5.16, 5.18, and 5.92 MeV was estimated from the known^{15,16} α -emission ratio of the 5.16-MeV level and the γ -ray yield from Table I. Since the reported α width for the 6.04-MeV level is not considered reliable,²⁰ an assumed α -emission ratio of 100:1 and the γ yield from Table I were used to compute the α -emission cross section from this level. The cross section for α emission from the levels discussed was estimated to be 434 mb, which, coupled with the measured γ -ray yield, gives a nonelastic cross section of 531 mb. The $(n, t2\alpha)$ reaction²⁶ and proton, α , and neutron emission to ground states of ^{10}Be , ^7Li , and ^{10}B are expected to contribute about 100 mb, so that the observed nonelastic cross section appears to be in reasonable agreement with that reported.²⁷

ACKNOWLEDGMENTS

The authors wish to express their sincere appreciation to J. B. Stout, Mrs. P. S. Buchanan, and G. H. Williams for their cooperation in making many of the measurements and assisting in the analysis of the data.

²⁶ J. R. Stehn, M. D. Goldberg, B. A. Magurno, and R. Wiener-Chasman, Brookhaven National Laboratory Report No. BNL-325, 2nd ed., Suppl. 2, 1964 (unpublished).

²⁷ M. H. MacGregor, W. P. Ball, and R. Booth, Phys. Rev. **108**, 726 (1957).